

Supplementary Information

Stacking of Colors in Exfoliable Plasmonic Superlattices

Mahsa Jalali,^{a,∇} Ye Yu,^{a,∇} Kaichen Xu,^b Ray Jia Hong Ng,^{a,c} Zhaogang Dong,^c Liancheng Wang,^a Saman Safari Dinachali,^{a,d} Minghui Hong*^b and Joel K. W. Yang*^{a,c}

^a Engineering Product Development, Singapore University of Technology and Design, 8 Somapah Road, Singapore 487372

^b Department of Electrical and Computer Engineering, National University of Singapore, Singapore 117576

^c Institute of Materials Research and Engineering, Agency for Science, Technology and Research (A*STAR), 2 Fusionopolis Way, #08-03 Innovis, Singapore 138634

^d Department of Materials Science and Engineering, Massachusetts Institute of Technology, Cambridge, Massachusetts 02139, United States

[∇] M. J. and Y. Y. contributed equally to this work

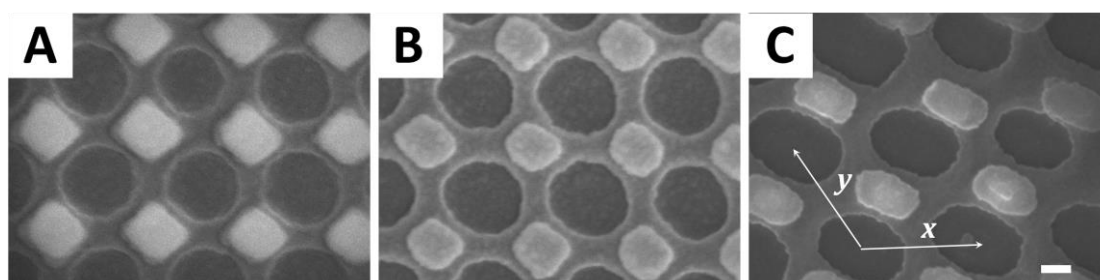


Figure S1. SEM images showing the three-tiered plasmonic superlattices with varied structural parameters: (A) $d=220$ nm, $a=178$ nm; (B) $d=250$ nm, $a=170$ nm; and (C) $d=280$ nm and 180 nm, $a=200$ nm and 100 nm along long and short axis, respectively. Pitch (P) was held constant of 350 nm throughout the experiments. The corresponding optical microscope images of (A,B,C) are shown in Figure 2H, I, J, respectively. Scale bar: 100 nm.

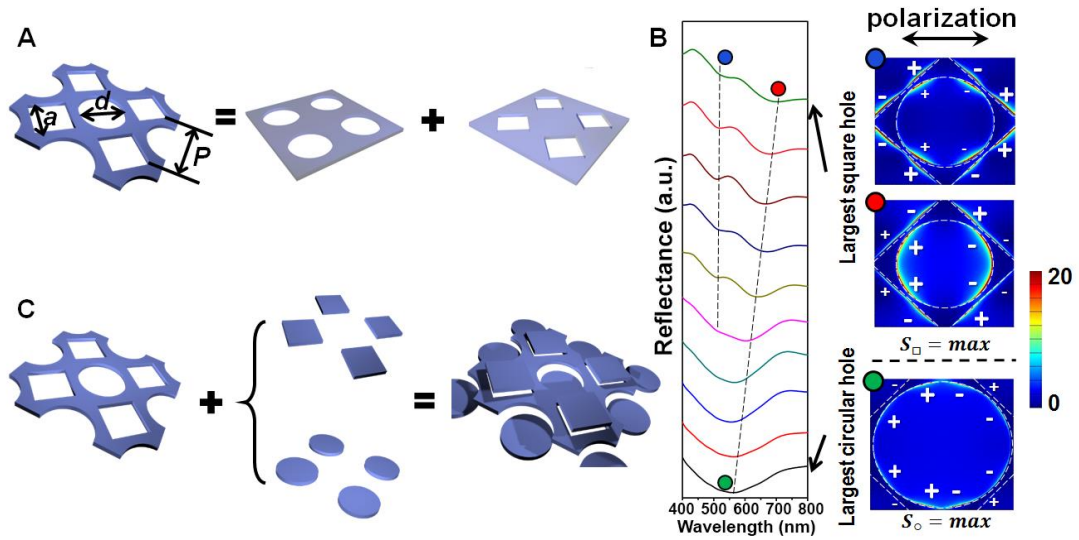


Figure S2. Illustration of the plasmonic superlattice. (A) Nanohole super-array with two sets of holes and (B) the corresponding calculated reflectance spectra (left panel) with varied structural parameters, along with the normalized electric field distribution $|E/E_0|^2$ plots of the unit cell (right panel). The structural parameters are as followed: pitch (P)=350 nm; diameter (d) of circular hole ranging from 240 to 332 nm; and edge size (a) of square hole ranging from 138 to 235 nm with $a+d$ held constant. (C) The vertical stacking of plasmonic superlattice showing the combination of nanohole super-array from (A) and two sets of disk arrays to form the 3-tier stacked structure.

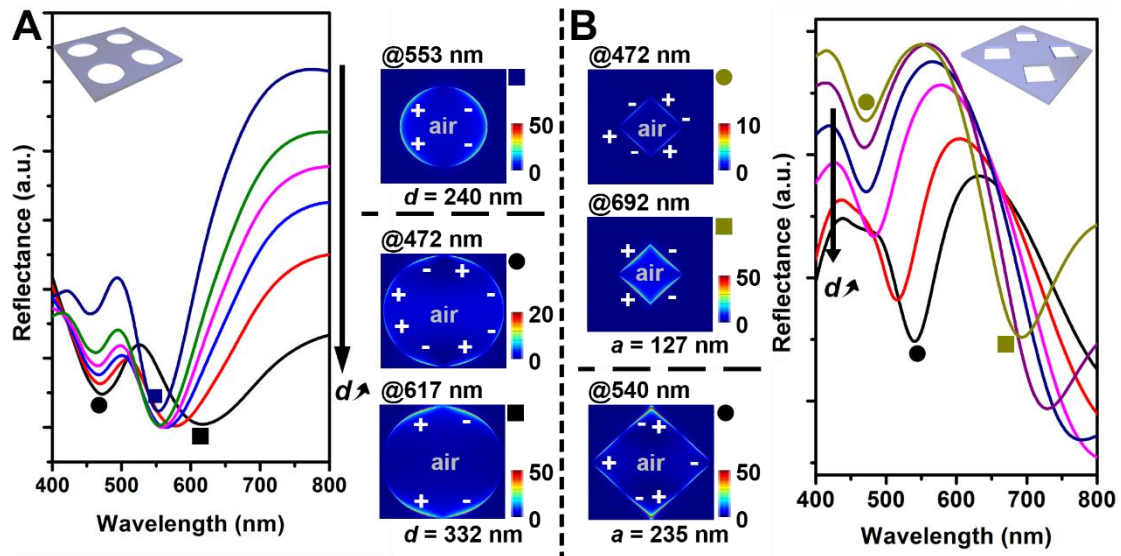


Figure S3. Comparison of simulated spectra between circular nanohole arrays (A) and square nanohole arrays (B) showing the distinguish contribution of holes regarding to the shape of the holes. Insets in both (A) and (B) indicate the related aluminum nanohole arrays where the photoresist structure and substrate are omitted for clear demonstration. Thickness of aluminum layer is 20 nm. Polarization direction is horizontal. Diameters of circular holes are: 240 nm (dark blue); 271 nm (green); 286 nm (magenta); 300 nm (blue); 316 nm (red); and 332 nm (black), respectively. Edge sizes of square holes are: 127 nm (dull yellow); 151 nm (dark purple); 175 nm (dark blue); 200 nm (magenta); 223 nm (red); and 235 nm (black), respectively. Two columns in the middle present the calculated electric field distribution ($|E/E_0|^2$) of the nanohole arrays with both the largest and smallest hole sizes at the corresponding dip positions, which were marked by ● and ■ symbols.

The two sets of nanohole arrays were analyzed separately, as shown in **Figure S3**. Series of spectra for both arrays show red-shift, along with charges re-distributed with increasing hole size, indicating a change of resonance modes in both nanohole arrays. We take the largest and smallest hole sizes of both sets as an example to show the electric field distribution, as shown in Figure S2. Simulated charge distribution charts of both nanohole arrays suggest the excitation of high-order bright modes of resonance, *i.e.* dipolar and hexapolar resonances.

Based on the resonance modes supported in the two sets of nanohole arrays, the hybridization of plasmonic resonance modes in the nanohole super-array shown in Figure 1 can be understood. The charge distributions at the two dips marked by blue and red in Figure S2 (upper right panel) indicate “bonding” plasmonic mode at a longer wavelength (red marker) and “anti-bonding” mode at a shorter wavelength (blue marker) of dipolar and hexapolar resonances. From the hybridization model, the charge distribution at the broad dip marked by green in Figure S2 (lower right panel) is likely a degenerate mode consisting of the hexapolar bonding and dipolar anti-bonding modes.

Figure S4 also provides similar results where we keep square holes with the largest size ($a=235$ nm) and reduce the size of circular holes from the diameter of 240 nm to 150 nm. The two dips within visible range show constant red-shift while the plasmonic hybridization modes stay the same. We further compared the spectra profiles with and without circular hole array, which are shown in **Figure S5**, indicating a redshift of 30 nm with the co-existence of circular hole array. The existence of plasmonic nanohole super-array leads to a complex plasmonic hybridization system where high-order modes of resonances can be excited and hybridized.

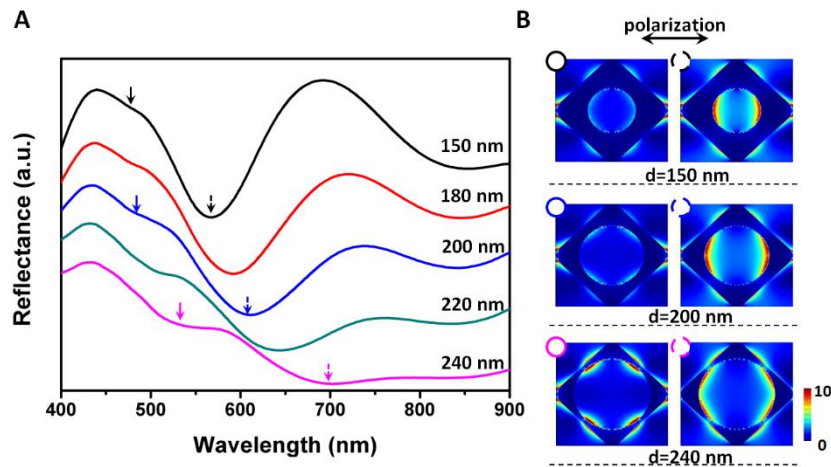


Figure S4. (A) Simulated reflectance spectra of nanohole super-array structure with maximum square hole size and varied circular hole size. The diameter of circular hole was varied from 150 nm to 240 nm while fixing the edge size of square at 170 nm. (B) Calculated electric field distribution $|E/E_0|^2$ at the reflectance dips indicated respectively with arrows and circles of same color and line type. Thickness of aluminum was 20 nm. The charge distributions for the nanohole super-array are in consistent with the one with the largest square hole shown in Figure 1B, regardless of different sizes of the circular hole here.

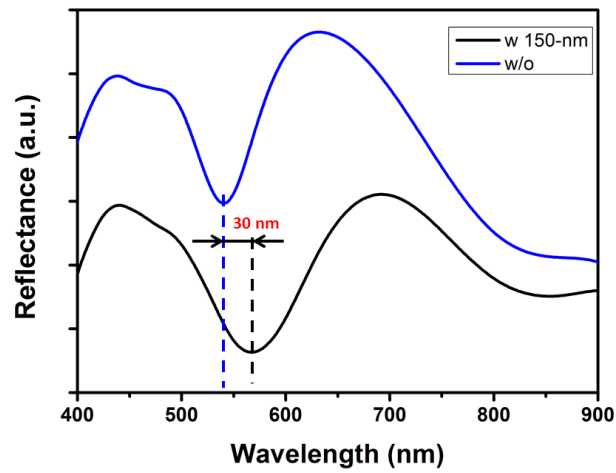


Figure S5. Simulated reflective spectra of square nanohole array (blue line) and nanohole superlattice with same size of square hole (edge size: 235 nm) and circular hole (black line) with a diameter of 150 nm. The existence of circular hole provides a red-shift of dip from 540 nm (blue line) to 570 nm (black line).

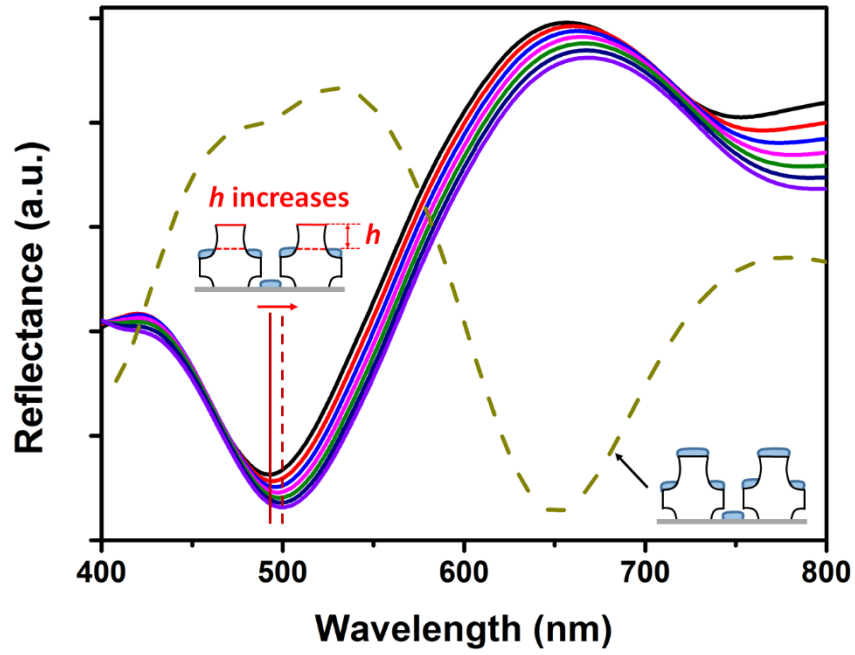


Figure S6. Simulated reflective spectra of three-tiered plasmonic superlattice structures with top layer removed and height of square posts (h) varies from 0 to 30 nm in step of 5 nm. Insets indicate the corresponding structures. Light blue part represents the deposited aluminum (20 nm). Red arrow indicates the spectrum red-shifts when h was increasing. Note that the dip positions are blue-shifted for ~ 25 nm compared with the ones in Figure 4, which is due to the difference in the overall height used in simulations.